Selected Papers of The Society of Naval Architects of Korea, Vol. 1, No.1, 1993. pp. 4~14.

Numerical Methods for Wave Response in Harbor

D.J. Kim* and K.J. Bai**

(From T.S.N.A.K., Vol.25, No.3, 1988)

Abstract

A natural and an artificial harbor can exhibit frequency (or period) dependent water surface oscillations when excited by incident waves. Such oscillations in harbors can cause significant damages to moored ships and adjacent structures. This can also induce undesirable current in harbor. Many previous investigators have studied various aspects of harbor resonance problem.

In the present paper, both a localized finite element method(LFEM) which is based on the functional constructed by Chen & Mei(1974) and Bai & Yeung(1974) and an integral equation method which was used by Lee(1969) are applied to harbor resonance problem. The LFEM shows computationally more efficient than the integral equation method. Our test results show a good agreement compared with other results. In the present computations, specifically two harbor geometris are treated here. The present method by LFEM can be extended to a fully three dimensional harbor problem.

1. Introduction

The knowledge of the wave responses in a harbor due to an incident wave is prerequisite for the safety of the anchored ships and offshore structures in the harbor. There are many cases of severe damages on the anchored ships due to the heavy storms. Accordingly there has been a growing need to develop a rational and efficient prediction method for the motion responses of the anchored ship and offshore structures in a harbor. This prediction method can also provide a valuable knowledge in the harbor resonance and guidelines for a harbor design.

During last twenty years there have been many investigations on a harbor resonance and wave responses in a harbor. For example, Kravtchenko & Mcnown [1] investigated an eigenvalue problem for a closed basin. Lee [2], Hwang & Tuck [3] and Mattioli [4] treated harbor oscillations by a method of integral equation. As another method of solution, Berkhoff [5, 6], Chen & Mei [7] and Bettes & Zienkiewicz [8] applied finite element methods to the problem. There were many investigations on a rather special harbor geometries, e.g., a rectangular or circular shapes where a more mathematical analysis is possible. However, this method has a severe limitation in

* Member, ADD Jinhae
** Member, Seoul National University

the application for a general harbor geometry.

In the present paper, we employed the localized finite element method which was successfully applied to water-wave problems by Bai & reung [9] and Kil [10]. By introducing a linear shallow-water theory, the problem is reduced to a two dimensinal problem on a horizontal plane. We also made another set of computations based on an integral equation. These two sets of computed results are compared and discussed. We also discussed on the harbor resonance and harbor paradox previously discussed by Miles & Munk [11].

2. Mathematical Formulation

2.1 Linear Shallow Water Theory

As in Fig. 1, by assuming that the bottom topography has a mild slope, one can obtain the following equations in terms of velocity potential $\phi(x,y)$ (See Berkhoff [5, 6] or Mei [12]) :

$$\nabla \cdot (C C_g \nabla \phi) + \omega^2 \frac{C_g}{C} \phi = 0 \tag{1}$$

$$\omega^2 = gk \tanh kh \tag{2}$$

ω

$$C = \frac{\omega}{k}$$

$$C_g = nC$$

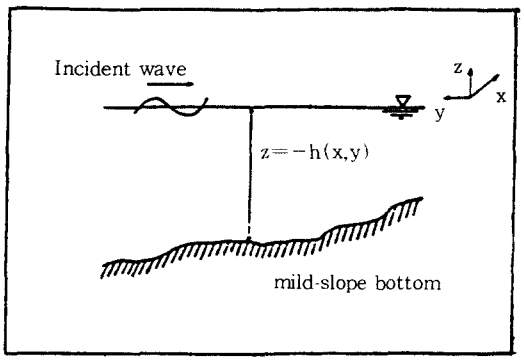

Fig. 1 Coordinate system and bottom topography

$C = \omega/k$ the phase velocity, and $C_g = nC$ the group velocity. Here

$$n = \frac{1}{2}\left(1 + \frac{2kh}{\sinh 2kh}\right)$$

By assuming kh is a small order of 1, i.e., $kh \ll 1$, we obtain n=1 and

$$C = C_g = \sqrt{gh} \tag{3}$$

By using this relation Equations (1) and (2) become

$$\nabla \cdot (h \nabla \phi) + \frac{\omega^2}{g} \phi = 0 \tag{4}$$

$$\omega^2 = gk^2 h \tag{5}$$

Equation (4) can be further reduced to following two-dimensional Helmholtz (or Weber) equation for a constant depth :

$$\nabla^2 \phi + k^2 \phi = 0 \tag{6}$$

$$\omega^2 = gk^2 h \tag{7}$$

2.2 Governing Equation and Boundary Conditions

The coordinate system and harbor configuration are given in Fig. 2. The water depth in the harbor is denoted by h(x,y). We assume that all the boundaries are vertical wall-sided and the coastline boundary gives a perfect reflection. Under usual assumptions made in the scope of the potential theory, the motion is assumed to be time harmonic with the frequency of the incident waves. Furthermore, the water depth outside of the harbor is assumed to be constant. The entire fluid domain is now divided into two sub-domains, i.e., (Ω_1 and Ω_1 as shown in Fig. 2. The boundary J denotes the juncture boundary of the two sub-domains. Now we can express the original problem in the following two problems defined in each sub domains. Here $\phi(x,y)$ is defined in Ω_1,

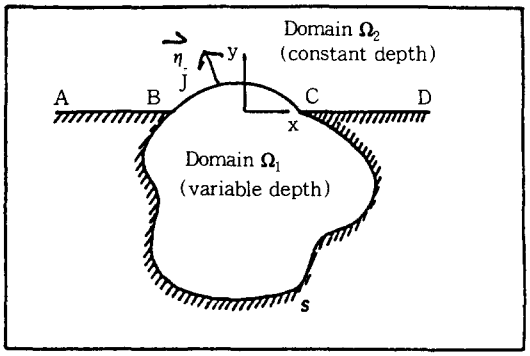

Ω_1 : variable depth
Ω_2 : constant depth
S : solid boundary inside the harbor
J : matching boundary
AB & CD : coastline

Fig. 2 Harbor model configuration

where i=1, 2. In the harbor, i.e., the sub domain, Ω_1, we obtain

$$\nabla \cdot (h\nabla \phi_1)+\frac{\omega^2}{g}\phi_1=0 \qquad \text{in } \Omega_1 \qquad (8)$$

$$\frac{\partial \phi_1}{\partial n}=0 \qquad \text{on S} \qquad (9)$$

In the outer domain, Ω_2, we obtain

$$\nabla^2\phi_2+k^2\phi_2=0 \qquad \text{in } \Omega_2 \qquad (10)$$

$$\frac{\partial \phi_2}{\partial n}=0 \qquad \text{on AB and CD} \qquad (11)$$

$$\lim_{r2\to\infty} \phi_2 \approx \phi_0 \qquad r^2=x^2+y^2 \qquad (12)$$

$$\phi_2=\phi_0+\phi_s$$
$$\phi_0=\phi_i+\phi_r \qquad (13)$$

Here ϕ_i denotes the incident-wave potential, ϕ_r the wave potential due to the perfect reflection along the coastline boundary, i.e., the coaslines denoted by AB and CD, and ϕ_s the scattered wave potential due to the presence of the harbor. Along the juncture boundary J, we require.

$$\phi_1=\phi_2 \qquad (14)$$

and

$$\frac{\partial \phi_1}{\partial n}=\frac{\partial \phi_2}{\partial n} \qquad (15)$$

Here the normal vector n is taken outward in Ω_1, and inward in Ω_2.

Since we assumed a perfect reflection along the coastline AB and CD, the sum of incident and reflected waves, denoted by ϕ_0 should satisfy.

$$\frac{\partial \phi_0}{\partial n}=\frac{\partial \phi_0}{\partial y}=0 \qquad \text{on AB and CD} \qquad (16)$$

Then Equations (10) through (13) reduce to the following equations in terms of the scattered velocity potential, ϕ_s :

$$\nabla^2\phi_s+k^2\phi_s=0 \qquad \text{in } \Omega_2 \qquad (17)$$

$$\frac{\partial \phi_s}{\partial n}=0 \qquad \text{on AB and CD} \qquad (18)$$

$$\lim_{r2\to\infty} \phi_s \approx 0 \qquad (19)$$

The solution of Equation (17) through (19) is $\frac{1}{2i}H_0^{(1)}(kr)$ where H is the Hankel function.

2.3 Amplification Factor

It is convenient to define an amplification factor to describe the wave response in a harbor. We define the amplication factor, R, as the ratio of the wave amplitude in the harbor to the amplitude of the standing wave, ϕ_0, which is obtained by assuming the harbor entrance is closed. This can be written as

$$R=\frac{|\bar{\eta}_1(x,y,t)|_{max}}{|\bar{\eta}_1(x,y,t)|_{max}+|\eta_r(x,y,t)|_{max}} \qquad (20)$$

Here $\eta_1(x,y,t)$ denotes the wave elevation and the subscripts, 1, i, and r are same as those de-

fined previously in the velocity potential functions. If we represent

$$\bar{\eta}_1(x,y,t) = Re\{\eta_1(x,y)e^{-i\omega t}\} \tag{21}$$

$$\eta_i(x,y) = Ae^{-ik\{x\cos\alpha + y\sin\alpha)} \tag{22}$$

$$\eta_r(x,y) = \eta_i(x,-y) \tag{23}$$

where A is the ampitude of the incident waves, α the angle of incidence of the incoming wave measured from the x-axis, and k the wave number. Then Eq. (20) reduces to

$$R = |\frac{\eta_1(x,y)}{2A}| \tag{24}$$

3. Localized Finite Element Method

The key idea in the localized finite element method is combining the usual finite element method in the harbor sub domain and the expressions by the known analytic solution with unknown coefficients in the truncated infinite sub domain (outer sub domain) through matching along the juncture boundary. This method has been successfully applied to free surface wave problems in Ref. [9, 10].

3.1 Construction of Variational Functional

Following Bai & Yeung [9], Kil [10], and Mei [12], for a variational problem equivalent to Equations (8), (9), (14), and (15), a variational functional can be defined as

$$F\{\phi_1, \phi_2\} = \iint_{\Omega_1} \frac{1}{2}[h(\nabla\phi_1)^2 - \frac{\omega^2}{g}\phi_1^2]dxdy + \int_J h[(\frac{1}{2}\phi_2 + \phi_1)\frac{\partial\phi_2}{\partial n}]ds - \frac{1}{2}\int_J h(\frac{\partial\phi_0}{\partial n}\phi_s - \frac{\partial\phi_s\phi_0}{\partial n})ds \tag{25}*$$

Then an equivalent variational problem can be written as

$$\delta F\{\phi_1, \phi_2\} = 0 \tag{26}$$

In order to show that this variational problem is equivalent to the original boundary value problem, we substitute Eq. (25) into Eq. (26) and obtain

$$\delta F\{\phi_1, \phi_2\} = \iint_{\Omega_1}[h\nabla\phi_1\nabla\delta\phi_1 - \frac{\omega^2}{g}\phi_1\delta\phi_1]dxdy + \int_J h[(\frac{1}{2}\delta\phi_2 - \delta\phi_1)\frac{\partial\phi_2}{\partial n} + (\frac{1}{2}\phi_2 - \phi_1)\frac{\partial\delta\phi_2}{\partial n}]ds - \frac{1}{2}\int_J h(\frac{\partial\phi_0}{\partial n}\delta\phi_s - \frac{\partial\delta\phi_s}{\partial n}\phi_0)ds \tag{27}$$

By using Gauss theorem and integration by parts, the first term in Eq. (27) becomes

$$\iint_{\Omega_1} h\nabla\phi_1\nabla\delta\phi_1 dxdy = \iint_{\Omega_1}[\nabla\cdot(h\delta\phi_1\nabla\phi_1) - \delta\phi_1\nabla\cdot(h\nabla\phi_1)]dxdy - \iint_{\Omega_1}\delta\phi_1\nabla\cdot(h\nabla\phi_1)dxdy + \int_S h\delta\phi_1\frac{\partial\phi_1}{\partial n}ds + \int_S h\delta\phi_1\frac{\partial\phi_1}{\partial n}ds \tag{28}$$

Since ϕ_0 is known function and its variation is zero, we have

$$\delta\phi_s = \delta\phi_2 \tag{29}$$

By using Eq. (28) (29), Eq. (27) reduces to

$$\delta F\{\phi_1, \phi_2\} = -\iint_{\Omega_1}\delta\phi_1[\nabla(h\nabla\phi_1) - \frac{\omega^2}{g}\phi_1]dxdy + \int_J[\delta\phi_1(\frac{\partial\phi_1}{\partial n} - \frac{\partial\phi_2}{\partial n}) - \frac{\partial\delta\phi_2}{\partial n}(\phi_1 - \phi_2)]ds + \int_S h\delta\phi_1\frac{\partial\phi_1}{\partial n}ds \tag{30}$$

In deriving Eq. (30), the following relations (31) and (32) are used.

If we apply the Green theorem for ϕ_s and $\delta\phi_s$ in Ω_2, we obtain

* In the original paper(J. SNAK Vol.25, No.3) the last term in Equations (25) (27) and (33) was missing by mistake

$$\iint_{\Omega_2}[\delta\phi_s(\nabla^2\phi_s+\frac{\omega^2}{gh}\phi_s)-\phi_s\delta\nabla^2\phi_s+\frac{\omega^2}{gh}\phi_s]dxdy$$

$$+\int_{\partial\Omega_2}(\frac{\partial\phi_s}{\partial n}\delta\phi_s-\phi_s\frac{\partial}{\partial n}\delta\phi_s)\,ds=0 \qquad (31)$$

Here $\partial\Omega_2$ is the closed boundary of Ω_2, i.e., $\partial\Omega_2$ =J+AB+CD+C_R, and C_R denotes a semicircular boundary with the radius r as r goes to infinity for y>0. By using Equations (11), (12), (13), (18), and (19) in Eq. (31), we obtain.

$$\int_J(\frac{\partial\phi_s}{\partial n}\delta\phi_s-\phi_s\frac{\partial}{\partial n}\delta\phi_s)\,ds=0 \qquad (32)$$

From variational equation Eq. (30), one can recover the original boundary value problem.

3.2 Approximate Solution in the Harbor

In the previous section it was shown that in the variational problem equivalent to the original problem the functional F is defined only in Ω_1 and its boundary, i.e.,

$$F\{\phi_1,\phi_2\}=\iint_{\Omega_1}\frac{1}{2}[h(\nabla\phi_1)^2-\frac{\omega^2}{g}\phi_1^2]dxdy$$

$$+\int_J h[(\frac{1}{2}\phi_2-\phi_1)\frac{\partial\phi_2}{\partial n}]ds$$

$$-\frac{1}{2}\int_J h\frac{\partial\phi_0}{\partial n}\phi_s-\frac{\partial\phi_s}{\partial n}\phi_0]\,ds \qquad (33)$$

The variational problem,

$$\delta F\{\phi_1,\phi_2\}=0 \qquad (34)$$

is to find the functions which makes the functional stationary with respect to ϕ_1 and ϕ_2.

In the present variational method an advantage is to look for an approximate solution in a wider class of admissible function space since any function and its first derivative which are square integrable are admissible now due to the integration by parts used in the construction of the functional.

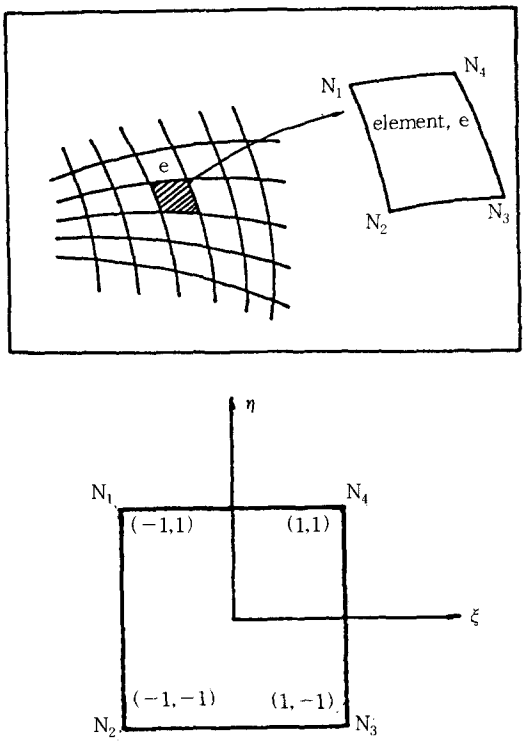

Master element(trial function basis)

Fig. 3 Finite element sobdivisions

The next step in the numerical procedure is to subdivide the harbor domain Ω_1 by finite number of finite elements as shown in Fig. 3. In the present computations, a four-node linear isoparametric element is used. By introducing trial function basis $N_i^e(x,y)$, (i=1,⋯,4) the velocity potential function $\phi_1(x,y)$ may be represented by

$$\phi_1=[N]^e\{\phi_1\}^{eT} \qquad (35)$$

where $[N]^e$ and $\{\phi_1\}^e$ are the trial function basis and the value of the potential function at the corresponding node, respectively. These can be expressed by

$$[N]^e=[N_1^e,\ N_2^e,\ N_3^e,\ N_4^e]$$

$$\{\phi_1\}^e=[\phi_{11}^e,\ \phi_{12}^e,\ \phi_{13}^e,\ \phi_{14}^e]$$

where the superscript T denotes the transpose of the vector and the trial function basis has the value of one at the corresponding node and zero at other nodes. Then the trial function can be written as

$$\phi_1 = \sum_{e=1}^{E} [N]^e \{\phi_1\}^e = \sum_{i=1}^{N} \phi_{1i} N_i(x,y) \tag{36}$$

where E and N are the total numbers of elements and nodes. Here $N_i(x,y)$ is the global basis function.

$$N_1 = \frac{1}{4}(1-\xi)(1+\eta)$$
$$N_2 = \frac{1}{4}(1-\xi)(1-\eta)$$
$$N_3 = \frac{1}{4}(1+\xi)(1-\eta)$$
$$N_4 = \frac{1}{4}(1+\xi)(1-\eta)$$

3.3 Representation of Approximate Solution in the Outer Sub domain

As mentioned in Section 2.1, the analytic solution for Equations (17) through (19) for the outer sub domain Ω_2 is Hankel function. As shown in Fig. 4. we denote a point on the matching boundary J by p(x,y). Then the pulsating source located at q(x′,y′) can be written as

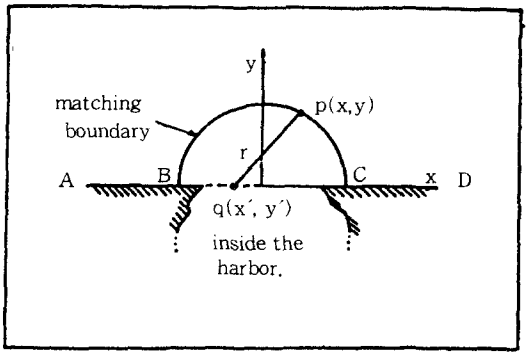

Fig. 4 Matching boundary & source distribution

$$G(p,q) = \frac{1}{2i} H_0^{(1)}(kr) = -\frac{1}{2}(Y_0 - iJ_0) \tag{37}$$

where $r=\{(x-x')^2+(y-y')^2\}^{1/2}$, and J_0 and Y_0 are Bessel functions of the first and second kinds, respectively. Instead of pulsating source distributions, one can also utilize Fourier-Bessel expansions as in Mei [12].

Any solution of ϕ_2 can be expressed by source distribution $\mu(q)$ along BC, i.e.,

$$\phi_2(p) = \phi_i(p) + \phi_r(p) + \phi_s(p) = \phi_i(p) + \phi_r(p) + \int \mu(p) G(p:q)\, ds \tag{38}$$

When we subdivide the harbor entrance BC by a number of small segments and assume a point source is located in each segment, we can approximate the potential as

$$\phi_2 = \phi_i + \phi_r + \sum_{i=1}^{M} \mu_{2i} \Psi_i(x,y) \tag{39}$$

where M is the number of source points and Ψ_i is source function at the i-th point.

3.4 Numerical Calculations

When we substitute the expressions in Eqs. (36) and (39) into Eq. (34), the following matrix equation can be obtained.

$$\frac{\partial F\{\phi_1, \phi_2\}}{\partial \phi_{1i}} = 0 \qquad i=1,\cdots,N$$
$$\frac{\partial F\{\phi_1, \phi_2\}}{\partial \mu_{2i}} = 0 \qquad i=1,\cdots,M \tag{40}$$

The final matrix equation has a nice and desirable property of being banded. A more details in the numerical procedures can be found in Kim [16].

4. Numerical Results and Discussions

Computations are made for two specific harbor geometries as shown in Fig. 5. Two different methods of solutions are developed : One by LFEM and the other is by the method of integral equation following Lee[2]. Throughout the computations the incoming wave is assumed to be incident normally to the coastlines, $\alpha=90°$. The computed results of the amplification factor (R) are shown with respect to the nondimensional wave number (KL) where L is the characteristic length of the harbor. The computed results are compared with those of Lee [2], Hwang & Tuck [3], Mattioli [4], and Mei [7]. For Model 1 computations are made for both with and without breakwater and also for depth variations. Model 2 is a simplified model for the Hangdong harbor in the City of Inchon, Korea. For this model the depth is assumed be constant.

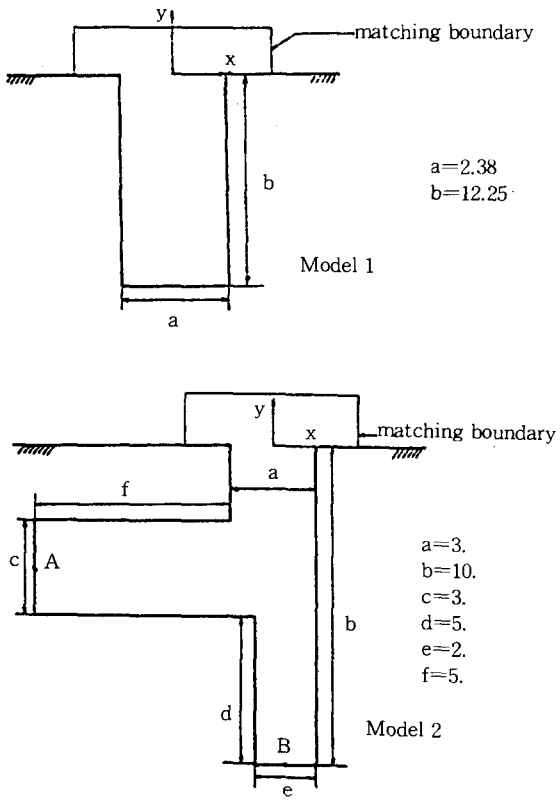

Fig. 5 Two harbor models

4.1 Comparisons between Results of Two Different Methods

In the computations by the LFEM, the number of elements was increased as the value of KL increased. In Fig. 6 and 7 the computed result of Model 1 for a constant depth by LFEM is compared with those obtained by other methods. Agreement is remarkable. It is found that in a simple geometry like Model 1, harbor resonance does not appear for KL > 5. However, in Model 2, the presence of the resonance was still pronounced when the wave number increases as shown in Fig. 15 and 16.

Fig. 8 shows the result of Model 1 for a linearly varying depth. It is of interest to note that as the water volume of the harbor decreases,

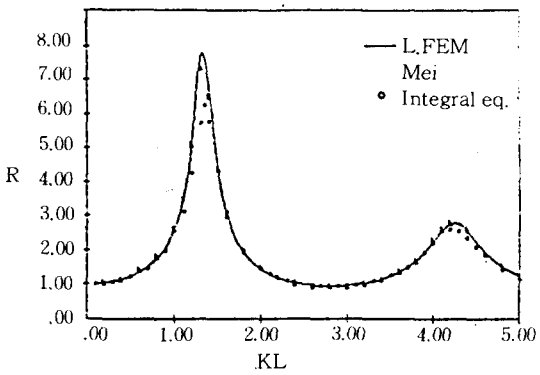

Fig. 6 [R] for constant bottom

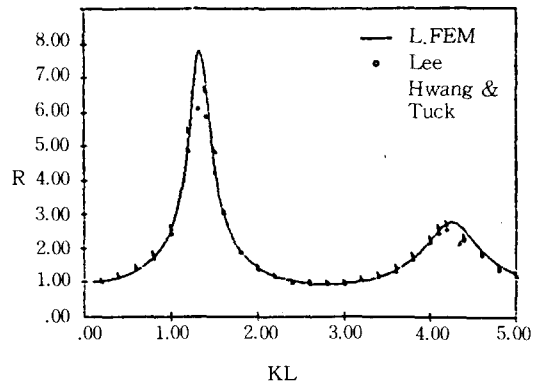

Fig. 7 [R] for constant bottom

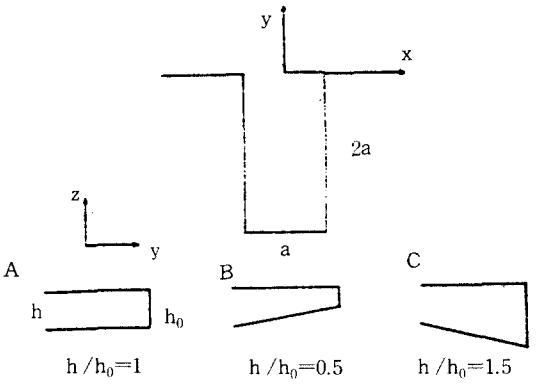

* Configuration of variable depth

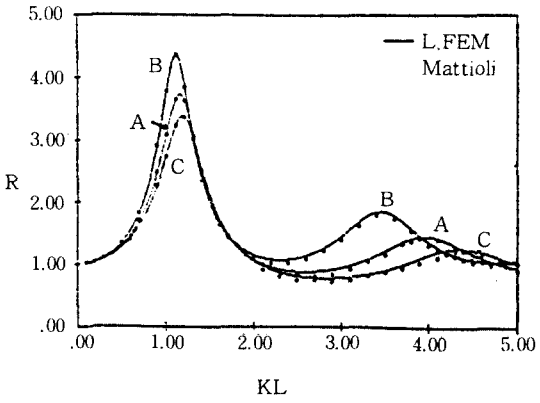

Fig. 8 [R] for linearly varying bottom

the resonant phenomenon becomes more pronounced.

4.2 Harbor with Breakwater

Fig. 9 shows the results of amplification factor for Model 1 without a breakwater while Fig. 10 shows those with a breakwater. The length of breakwater is a/4 and extended from both ends of the harbor entrance. The amplification factors are computed at two locations i.e., A and B as shown in the figures. Comparisons show that the values of R is larger in the case with a breakwater than those without it. This seemingly contradictory phenomena is called a harbor paradox and discussed by Miles & Munk [11] and Mei

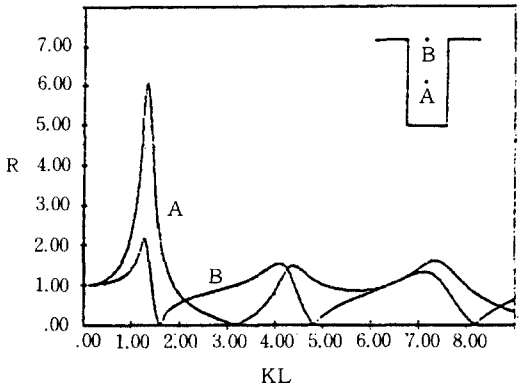

Fig. 9 [R] at point A & B

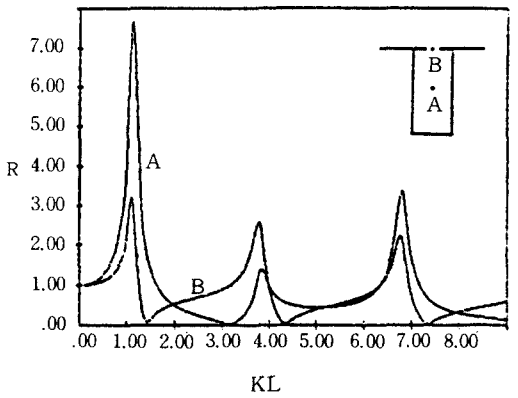

Fig. 10 [R] at point A & B(with breakwater)

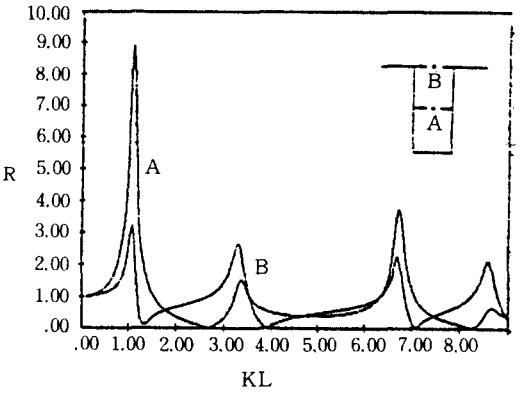

Fig. 11 [R] at point A & B with two breakwaters

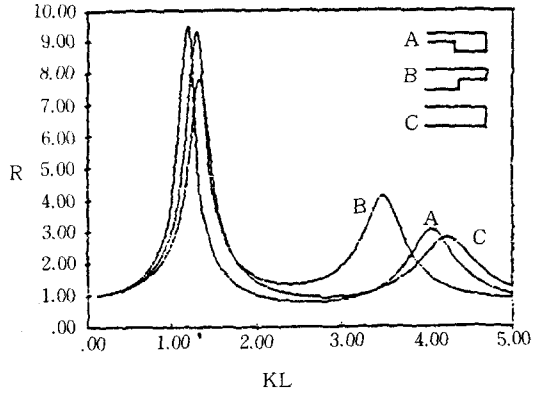

Fig. 12 [R] for stepped bottom

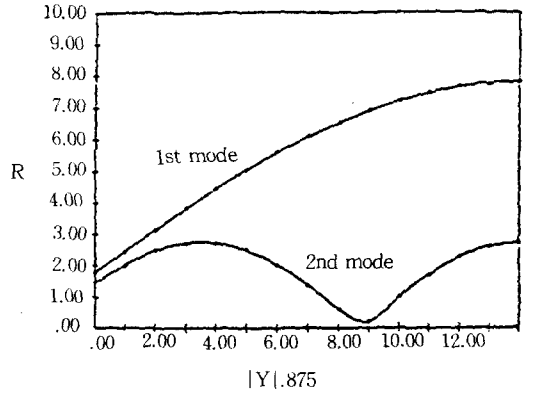

Fig. 13 [R] along the Y-axis
(for the case of Fig. 9 without breakwater)

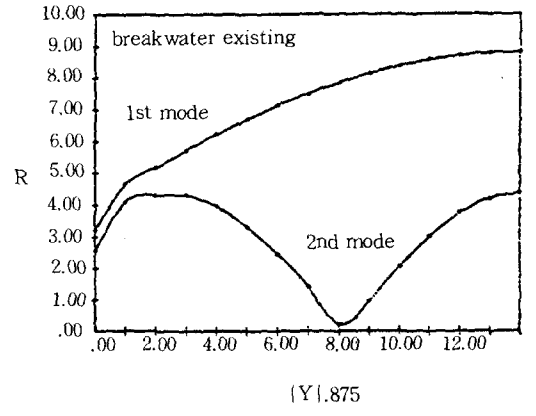

Fig. 14 [R] along the Y-axis with a breakwater
(for the case of Fig. 10)

[12]. This paradox can be explained by the fact that when the harbor entrance becomes smaller, then the incident wave energy entered into the harbor can not easily get out and is rather trapped.

Fig. 11 shows the results of amplification factors when a second breakwater is introduced in the mid section of the Harbor. It is of interest to note that the values of R becomes even more pronounced with two breakwaters.

Fig. 12 show the results for three stepped bottom topography. It should be noted that the water depth increases after the entrance, the amplification factor is more pronounced. This can be interpreted as a similar phenomena of harbor paradox.

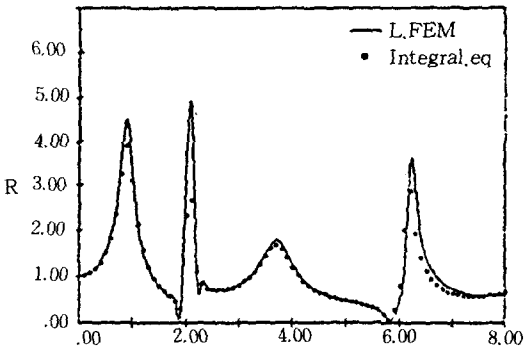

Fig. 15 [R] at point A, model 2

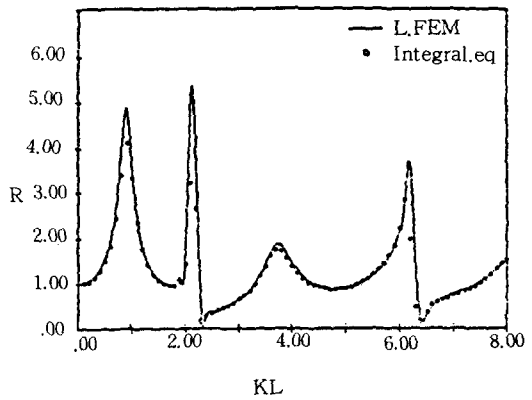

Fig. 16 [R] at point B, model 2

Fig. 13 and 14 show the amplification factors for the two lowest resonant modes versus the y-coordinate along the center lines for the cases treated in Fig. 9 and 10.

4.3 Convergence in Numerical Computations

Throughout the present computations, the number of element is taken at least ten per a wave length in order to guarantee a good resolution. In the computations by LFEM by distributing few point singularities between three and seven the results were very close to those of Mei [12] as shown in Fig. 6. However, when we increased the number of distributed source points without increasing the number of finite element along the matching boundary J, and computed results became less accurate. Specifically, this happened in the present calculations when the number of source points were taken more than 80% of the number of segments along the matching boundary. This loss of the accuracy by increasing the number of source points beyond the optimum number is presumably due to the fact that the information to be provided by relatively too few linear elements on J and by using numerical quadrature for the coupling integral terms is not sufficient to determine the too many unknowns for the source strengths.

Table 1 shows comparisons of computation times between LFEM and integral equation method. It should be noted that the computation (CPU) time required in the conventional method of integral equation takes approximately 4~15 times longer than that required in LFEM in the present computations.

Table 1 Comparison of computation time (MV8000 사용시)

	method	no. of segments	no. of matching boundary	no. of sources	C.P.U time
Model 1	LFEM	80	14	5	6 sec
	I.E.M	48	5	–	38 sec
Model 2	LFEM	216	22	5	23 sec
	I.E.M	69	5	–	75 sec

5. Concluding Remarks

The computational method by LFEM is developed for IBM PC XT & AT. It is shown that agreement is good between the results obtained by LFEM and those by other methods. Furthermore LFEM has computational effeciency over the method of integral equation as shown in the present results. The present method (LFEM) can be easily extended to treat general three-dimensional harbor geometry in a straightforward manner.

References

[1] Kravchenko, J. & Mcnown, J.S., "Seiche in Rectangular Port", *Quart. Appl. Math.* 13, 19–26, 1955.

[2] Lee, J.J., "Wave-Induced Oscillations in Harbors of Arbitrary Shape", Ph.D. thesis, Cal.Inst. Tech, 1969.

[3] Hwang, L.S. & Tuck, E.O., "On the Oscillations of Harbors of Arbitrary Shape", *J.Fluid Mech.* 42, 477–464, 1970.

[4] Mattioli, F., "Wave-Induced Oscillations in Harbors of Variable Depth", *Computers and Fluids*, 6, 161–172, 1978.

[5] Berkhoff, J.C.W., "Computation of Combined Refraction-Diffraction", *Proc. 13th nt. Conf. Coastal Engineering Vancouver*, Canada, 1972.

[6] Berkhoff, J.C.W., "Mathematical Models for Simple Harmonic Linear Water Waves-Wave Diffraction and Refraction", *Report on Mathematical Investigation*, Delft Hydraulics Laboratory, W163, 1976.

[7] Chen, H.S. & Mei, C.C., "Oscillations and Wave Force in a Man-Made Harbor in the Open Sea", *The 10th Naval Hydrodynamics Symposium*, Office of Naval Research, 1974.

[8] Bettes, P. & Zienkiwicz, O.C., "Diffraction and Refraction of surface wave using finite and infinite elements", *Int. Journal for Numerical Methods in Engineering*, Vol.12, 1271–1290, 1977.

[9] Bai, K.J. & Yeung, R., "Numerical Solutions of Free-Surface Flow Problems", *Proc. 10th Symp. Naval Hydrodynamics,* Office of Naval Research, 1974.

[10] Kil, H.K., "A Localized Finite Element Method for a Free Surface Wave Problem", MS Thesis, Seoul National University, Dept. of Naval Architecture, 1985.

[11] Miles, J. & Munk, W., "Harbor paradox. Journal of Waterways and Harbors Division", *ASCE,* No.2888, 1961.

[12] Mei, C.C., "The Applied Dynamics of Ocean Surface Waves", *John Wiley & Sons,* 1982.

[13] Baker, B.B. & Copson, E.T., "The Mathematical Theory of Huygens' Principle", Oxford University Press, 1950.

[14] Banaugh, R.P. & Goldsmith, W., "Diffraction of Steady Acoustic Waves by Surfaces of Arbitrary Shape", *J. Acoust. Soc. Am.* 35, 1950-1601, 1963.

[15] Becker, E.B., Carey, G.F. & Oden, J.T., "Finite Elements", Prentice-Hall, Inc. 1981.

[16] Kim, D.J., "Numerical Method for Wave Response in a Harbor", MS Thesis, Seoul National University, Dept. of Naval Architecture, 1987.